Dissipative Duct

1 Introduction

This example demonstrates the propagation of sound in a dissipative acoustic waveguide. A duct with a square cross-section is considered. The side walls are lined with a locally reacting sound absorbing material of impedance Z_w. Using this example, several interesting physical phenomena that occur in waveguides such as dispersion, cutoff frequencies of the various transverse modes, and attenuation of sound etc. are explained. Analytical solution is derived and compared with Coustyx solutions. Excellent agreement is observed.
This example makes extensive use of the scripting feature of Coustyx to model side wall impedance that varies with frequency, and in functions for computing the transverse eigenvalues for use in the analytical solution.

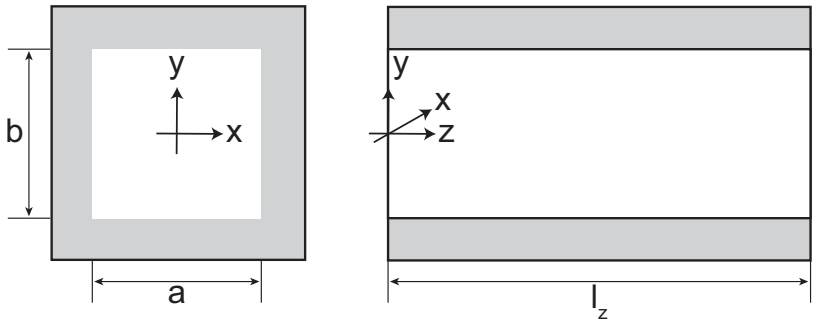

Figure 1: An acoustically lined duct of rectangular cross-section.

2 Problem Statement

A schematic of the dissipative duct is shown in Figure 1. The face at $z = 0$ is oscillates back and forth at a frequency ω, and a velocity amplitude U. At $z = l_z$, an anechoic termination boundary condition is applied. The duct is lined on all four sides with a 1-inch thick foam with a rigid backing. The excitation frequency $f = 1000\,\text{Hz}$, and the duct dimensions are 10 cm x 10 cm x 60 cm. The fluid medium inside the duct is air with a sound speed of $c = 343\,\text{m/s}$ and an ambient density of $\rho = 1.21\,\text{Kg/m}^3$. We are interested in the sound field inside the duct.
The real and imaginary parts of the normalized impedance $Z_w(\omega)/\rho c = R(\omega)/\rho c + iX(\omega)/\rho c$ of 1-inch thick foam with a rigid wall backing is obtained experimentally [1], and plotted in Figure 2. From Figure 2, it is seen that the real part of impedance $R(\omega)$ (called resistance) is always *positive*, as required for an energy absorber. Also, as noted in Pierce [2], typical acoustic liners are stiffness-controlled at low frequencies, and the acoustic reactance $X(\omega)$ is *large and positive* for small ω. This can be observed in Figure 2 as well.

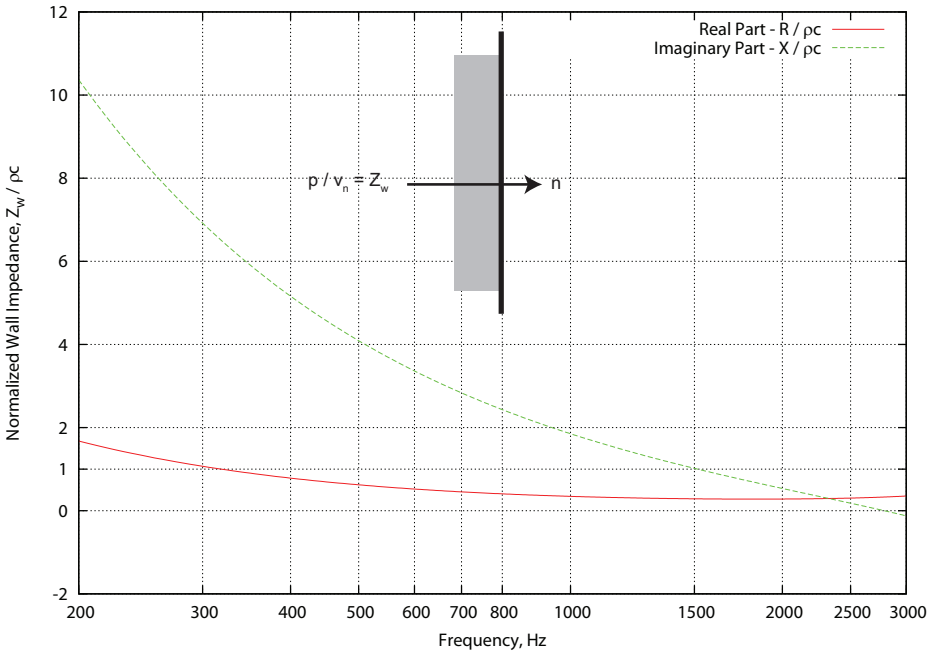

Figure 2: Normalized impedance of 1-inch thick foam with a rigid wall backing.

3 Analytical Solution

Our derivation of the analytical solution is similar to that of Munjal [3]. Our version differs from Munjal [3] with respect to the choice of the origin for the coordinate system. In our opinion choosing the center line of the duct to be (0,0) simplifies the presentation greatly, and the symmetric and anti-symmetric modes are very easily identifiable.
Employing the separation of variables, we look for a solutions of the form

$$p(x,y,z) = \left\{e^{ik_x x} + c_1 e^{-ik_x x}\right\}\left\{e^{ik_y y} + c_2 e^{-ik_y y}\right\}\left\{e^{ik_z z} + c_3 e^{-ik_z z}\right\} \tag{1}$$

The expressions for the pressure gradient are given by the following equations.

$$\frac{\partial p}{\partial x}(x,y,z) = ik_x\left\{e^{ik_x x} - c_1 e^{-ik_x x}\right\}\left\{e^{ik_y y} + c_2 e^{-ik_y y}\right\}\left\{e^{ik_z z} + c_3 e^{-ik_z z}\right\} \tag{2}$$

$$\frac{\partial p}{\partial y}(x,y,z) = ik_y\left\{e^{ik_x x} + c_1 e^{-ik_x x}\right\}\left\{e^{ik_y y} - c_2 e^{-ik_y y}\right\}\left\{e^{ik_z z} + c_3 e^{-ik_z z}\right\} \tag{3}$$

$$\frac{\partial p}{\partial z}(x,y,z) = ik_z\left\{e^{ik_x x} + c_1 e^{-ik_x x}\right\}\left\{e^{ik_y y} + c_2 e^{-ik_y y}\right\}\left\{e^{ik_z z} - c_3 e^{-ik_z z}\right\} \tag{4}$$

Euler's equation relates the acoustic particle velocity to the pressure gradient as follows:

$$u_x(x,y,z) = \tfrac{1}{ikZ_o}\tfrac{\partial p}{\partial x}(x,y,z); \quad u_y(x,y,z) = \tfrac{1}{ikZ_o}\tfrac{\partial p}{\partial y}(x,y,z); \quad u_z(x,y,z) = \tfrac{1}{ikZ_o}\tfrac{\partial p}{\partial z}(x,y,z) \tag{5}$$

The solution procedure is as follows: First the the transverse wavenumber k_x and coefficient c_1 are determined by satisfying the boundary conditions on faces $x = -a/2$ and $x = a/2$. The transverse wavenumber k_y is similarly determined. Once k_x and k_y are known, the value of propagation wavenumber k_z is given by $k_z = \sqrt{k^2 - k_x^2 - k_y^2}$.

3.1 Determination of Transverse Eigenmodes

The impedance boundary condition on the face $x = a/2$ yields

$$\frac{p(\frac{a}{2},y,z)}{u_x(\frac{a}{2},y,z)} = Z_w \tag{6}$$

This leads to

$$\frac{e^{ik_x\frac{a}{2}} + c_1 e^{-ik_x\frac{a}{2}}}{e^{ik_x\frac{a}{2}} - c_1 e^{-ik_x\frac{a}{2}}} = \frac{k_x}{k}\frac{Z_w}{Z_o} \tag{7}$$

The boundary condition on the face $x = -a/2$ yields

$$\frac{p(-\frac{a}{2}, y, z)}{-u_x(-\frac{a}{2}, y, z)} = Z_w \tag{8}$$

The negative sign for the velocity term in Equation 8 can be explained using the schematic in Figure 2. The convention followed for measuring impedance uses the component of velocity going *into* the acoustic liner, which is $-u_x$ in this case.
Equation 8 simplifies to

$$\frac{e^{-ik_x\frac{a}{2}} + c_1 e^{ik_x\frac{a}{2}}}{e^{-ik_x\frac{a}{2}} - c_1 e^{ik_x\frac{a}{2}}} = -\frac{k_x}{k}\frac{Z_w}{Z_o} \tag{9}$$

Let

$$A = e^{ik_x\frac{a}{2}}; \quad B = e^{-ik_x\frac{a}{2}}; \quad R = \tfrac{k_x}{k}\tfrac{Z_w}{Z_o} \tag{10}$$

Equation 7 simplifies to

$$\frac{A + c_1 B}{A - c_1 B} = R \tag{11}$$

and Equation 9 simplifies to

$$\frac{B + c_1 A}{B - c_1 A} = -R \tag{12}$$

Solving Equation 11 and Equation 12 for c_1 yields $c_1 = \pm 1$. $c_1 = 1$ yields symmetric transverse modes in the x-direction as the pressure variation $\left\{e^{ik_x x} + e^{-ik_x x}\right\}$ is symmetric about $x = 0$. Similarly $c_1 = -1$ yields anti-symmetric modes about $x = 0$ since the pressure variation $\left\{e^{ik_x x} - e^{-ik_x x}\right\}$ is an odd function.
The next step is the determination of the eigenvalues ($k_x a/2$) for the transverse symmetric and anti-symmetric modes.

3.1.1 Eigenvalues of Transverse Symmetric Modes

Solving Equation 7, given $c_1 = 1$ leads to the following transcendental equation for determination of the eigenvalue $k_x a/2$.

$$\frac{e^{ik_x\frac{a}{2}} + e^{-ik_x\frac{a}{2}}}{e^{ik_x\frac{a}{2}} - e^{-ik_x\frac{a}{2}}} = \frac{k_x}{k}\frac{Z_w}{Z_o} \tag{13}$$

$$\cot(\frac{k_x a}{2}) = i\frac{k_x}{k}\frac{Z_w}{Z_o} \tag{14}$$

$$\frac{\cot(\frac{k_x a}{2})}{\frac{k_x a}{2}} = i\frac{2}{ka}\frac{Z_w}{Z_o} \tag{15}$$

Equation 15 is solved using iterative techniques, such as the Newton-Raphson method to determine the symmetric eigenvalues $k_x a/2$.

3.1.2 Eigenvalues of Transverse Anti-Symmetric Modes

Solving Equation 7, given $c_1 = -1$ yields the eigenvalues for the anti-symmetric modes.

$$\frac{e^{ik_x\frac{a}{2}} - e^{-ik_x\frac{a}{2}}}{e^{ik_x\frac{a}{2}} + e^{-ik_x\frac{a}{2}}} = \frac{k_x}{k}\frac{Z_w}{Z_o} \tag{16}$$

$$i\tan(\frac{k_x a}{2}) = \frac{k_x}{k}\frac{Z_w}{Z_o} \tag{17}$$

$$\frac{\tan(\frac{k_x a}{2})}{\frac{k_x a}{2}} = -i\frac{2}{ka}\frac{Z_w}{Z_o} \tag{18}$$

The following observations can be made from Equation 15 and Equation 18.

- If Z_w were purely reactive, the right hand sides of Equation 15 and Equation 18 are real valued, and hence the eigenvalue $k_x a/2$ will be real. In this case, $k_z = \sqrt{k^2 - k_x^2 - k_y^2}$ will be either real or purely imaginary.

  For a real valued k_z we have wave traveling down the duct without any attenuation, while purely imaginary k_z corresponds to the case where the excitation frequency is below the cutoff frequency for the given transverse mode, and thus leads to an evanescent wave. Thus a pipe with yielding walls, where Z_w is purely reactive as it is stiffness controlled, *will not cause any attenuation.*

- The eigenvalues $k_x a/2$ are dependent on the excitation frequency, as the wavenumber k is explicitly present of the right hand side of the eigenvalue equations. Hence in a multi-frequency analysis, the eigenvalues need to be recomputed for every analysis frequency.

- The convergence of the iterative techniques for solving the eigenvalue equations (Equation 15 and Equation 18) depends heavily on the choice of a good initial guess. Initial guesses that are not sufficiently close to the solution cause the eigenvalue solver to diverge. Using initial guesses that correspond to the transverse eigenvalues with rigid walls ($Z_w = \infty$) with a small negative imaginary part, seems to work well.

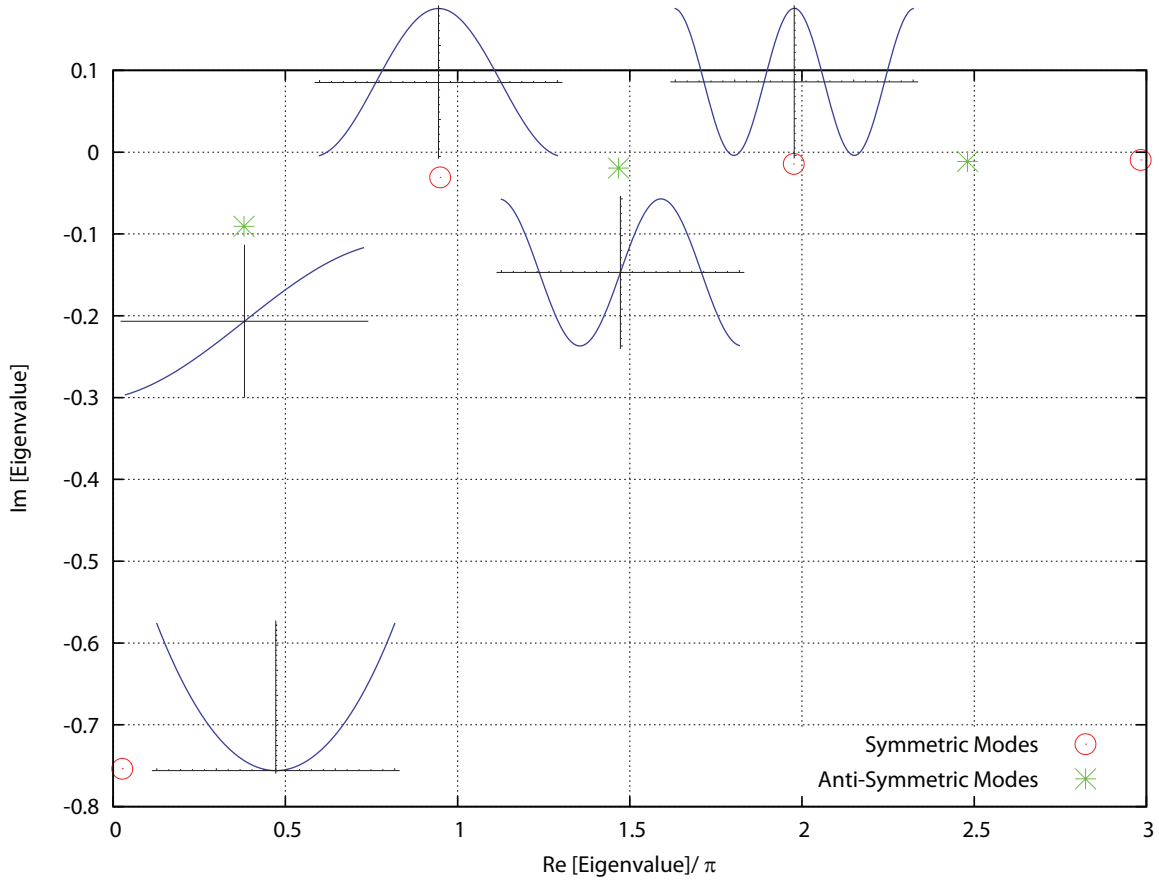

Figure 3: Transverse eigenvalues and modes for the square duct at a frequency of $f = 1000\,\text{Hz}$.

Figure 3 shows the symmetric and anti-symmetric eigenvalues distributed in the complex plane. The mode shapes associated with an eigenvalue are plotted near it. The computed eigenvalues for the given side-wall impedance Z_w are close to the ones for a rigid walled duct, especially for the higher eigenvalues.
Table 1 shows the eigenvalues $k_{x,m}a/2$ and transverse wavenumbers $k_{x,m}$ for the first sixteen modes ($m = 0, \ldots 15$). In Table 1, the index m represents the number of nodal points for the sound pressure mode shape in the x-direction.

Table 1: Transverse eigenvalues and wavenumbers $k_{x,m}$ at 1000 Hz.

m	$\Re(k_{x,m}a/2)$	$\Im(k_{x,m}a/2)$	$\Re(k_{x,m})$	$\Im(k_{x,m})$
0	0.082	-0.753	1.64	-15.07
1	1.193	-0.091	23.868	-1.814
2	2.983	-0.031	59.657	-0.615
3	4.609	-0.02	92.182	-0.391
4	6.206	-0.014	124.127	-0.289
5	7.793	-0.011	155.854	-0.23
6	9.374	-0.01	187.477	-0.191
7	10.952	-8e-3	219.04	-0.163
8	12.528	-7e-3	250.564	-0.143
9	14.103	-6e-3	282.066	-0.127
10	15.678	-6e-3	313.55	-0.114
11	17.251	-5e-3	345.022	-0.103
12	18.824	-5e-3	376.484	-0.095
13	20.397	-4e-3	407.938	-0.087
14	21.969	-4e-3	439.388	-0.081
15	23.542	-4e-3	470.832	-0.076

Each transverse mode (m, n) propagates down the duct at a propagation wavenumber $k_{z,m,n}$ given by $k_{z,m,n} = \sqrt{k^2 - k_{x,m}^2 - k_{y,n}^2}$. The propagation wavenumbers for the first five transverse mode combinations is shown in Table 2. *The imaginary part of $k_{z,m,n}$ is responsible for the attenuation of the wave amplitude. This is the basic working principle behind dissipative mufflers.*
From Table 2 it seen except for (0,0), (1,0) and (0,1) modes, all the other modes have very high attenuation rates and decay rapidly. If the duct were to be lined with rigid walls, the excitation frequency of $f = 1000$ Hz is below the cutoff frequency for the higher order modes, leading to evanescent waves.

Table 2: Propagation wavenumbers $k_{z,m,n}$ for various transverse modes at $f = 1000$ Hz.

m,n	$n=0$		$n=1$		$n=2$		$n=3$		$n=4$	
	$\Re$	$\Im$	$\Re$	$\Im$	$\Re$	$\Im$	$\Re$	$\Im$	$\Re$	$\Im$
$m=0$	28.06	1.76	8.05	8.44	1.12	54.77	0.68	89.09	0.50	121.85
$m=1$	8.05	8.44	3.05	28.40	1.30	61.57	0.85	93.43	0.63	125.05
$m=2$	1.12	54.77	1.30	61.57	0.89	82.35	0.67	108.26	0.53	136.49
$m=3$	0.68	89.09	0.85	93.43	0.67	108.26	0.56	129.07	0.47	153.52
$m=4$	0.50	121.85	0.63	125.05	0.53	136.49	0.47	153.52	0.41	174.58

Modes (1,0) and (0,1) are anti-symmetric modes. They will not be excited by the specified velocity distribution at $z = 0$, which is uniform. Hence the mode (0,0), the *first symmetric mode* is also the *least attenuated mode*, and hence **the dominant mode in the response**.
From the above discussion, it is clear that a very good approximation can be obtained using a one term eigensolution.

$$p(x, y, z) = C \left\{ e^{ik_{x,0}x} + e^{-ik_{x,0}x} \right\} \left\{ e^{ik_{y,0}y} + e^{-ik_{y,0}y} \right\} e^{ik_{z,0,0}z} \tag{19}$$

$$u_z(x, y, z) = \frac{1}{ikZ_o} \frac{\partial p}{\partial z}(x, y, z) = C \frac{1}{Z_o} \frac{k_{z,0,0}}{k} \left\{ e^{ik_{x,0}x} + e^{-ik_{x,0}x} \right\} \left\{ e^{ik_{y,0}y} + e^{-ik_{y,0}y} \right\} e^{ik_{z,0,0}z} \tag{20}$$

The unknown coefficient C is determined to satisfy the velocity boundary condition at $z = 0$. Instead of satisfying the velocity boundary condition point-wise at $z = 0$, the coefficient C is determined by matching the *volume velocity* from Equation 20 to that from the prescribed boundary condition.

$$Ua^2 = Ca^2 \frac{1}{Z_o} \frac{k_{z,0,0}}{k} 4 \left(\frac{\sin \frac{k_{x,0}a}{2}}{\frac{k_{x,0}a}{2}} \right)^2 \tag{21}$$

The expression for the pressure field inside the duct is given by

$$p(x,y,z) = \frac{UZ_o}{4}\frac{k}{k_{z,0,0}}\left(\frac{\frac{k_{x,0}a}{2}}{\sin\frac{k_{x,0}a}{2}}\right)^2 \left\{e^{ik_{x,0}x} + e^{-ik_{x,0}x}\right\}\left\{e^{ik_{y,0}y} + e^{-ik_{y,0}y}\right\} e^{ik_{z,0,0}z} \tag{22}$$

$$p(x,y,z) = UZ_o\frac{k}{k_{z,0,0}}\left(\frac{\frac{k_{x,0}a}{2}}{\sin\frac{k_{x,0}a}{2}}\right)^2 \cos\left(k_{x,0}x\right)\cos\left(k_{y,0}y\right) e^{ik_{z,0,0}z} \tag{23}$$

Equation 23 is the analytical solution for the pressure field inside the duct using a one term modal summation (first symmetric mode).
Two observations can be made from Equation 23.

1. The variation of sound pressure at a given z is of the the form $\cos\left(k_{x,0}x\right)\cos\left(k_{y,0}y\right)$. Since the first transverse eigenvalue $k_{x,0}a/2$ is such that $\Re(k_{x,0}a/2) \approx 0$, $\cos(k_{x,0}a/2) \approx 1$. Hence, at any cross-section, the *maximum sound pressure occurs at a corner.*

2. The excitation starting out as a plane-wave at $z = 0$, takes the shape of the first symmetric mode as it travels along the duct, due to rapid attenuation of the higher order modes.

Equation 23 is used for comparisons with the numerical solution from Coustyx.

3.1.3 Termination Condition

At the end $Z = l_z$, an anechoic termination boundary condition is desired. Modeling the end impedance as the medium characteristic impedance $Z_0 = \rho c$ would be an *approximation that is valid only at high frequency, due to the dispersion characteristics of the waveguide, since* $c_{phase} = k_z/\omega = c_{phase}(\omega)$. A more precise way of modeling the anechoic termination boundary condition is to use Equation 23 directly, and compute the ratio of pressure to velocity. This is given as

$$\frac{p(x,y,z)}{u_z(x,y,z)} = Z_o\frac{k}{k_{z,0,0}} \tag{24}$$

Equation 24 is applied as the boundary condition in the Coustyx model $z = l_z$ using the Coustyx scripting feature, as the right hand side of Equation 24 is frequency dependent.

4 Coustyx Model

The Coustyx model of the 10 cm x 10 cm x 60 cm duct contains 2600 linear elements, 2602 coordinate nodes, 2602 pressure nodes, and 2926 pn nodes. The element size is 1 cm x 1 cm. Using the $\lambda/6$ thumb rule for element size, the boundary element model is valid till a frequency of 5053 Hz. The number of pn variable nodes is different from the number of pressure nodes due to the duplication of the pn nodes at the edges and corners of the duct where the element normals are discontinuous. The fluid medium in the duct is air with sound speed $c = 343\,\mathrm{m/s}$ and mean density $\rho = 1.21\,\mathrm{kg/m^3}$. The characteristic impedance of air $Z_o = \rho c = 415.03\,\mathrm{Rayl}$.
We apply an uniform velocity boundary condition of amplitude $U = 1\,\mathrm{m/s}$ at $z = 0$, at a frequency $f = 1000\,\mathrm{Hz}$. Anechoic termination boundary condition as given by Equation 24 is applied at $z = l_z$, and the frequency dependent acoustic liner impedance on the side walls of the duct. Modeling of the boundary conditions is made very easy by the advanced scripting capabilities of Coustyx.
The `Context Script` contains functions for computing the impedance of the acoustic liner at any frequency, and analytical solutions for the sound pressure and velocity. Functions that are placed in the `Context Script` have a global scope, and can be used inside any `Analysis Sequence`.
Using this example, we are interested in learning about the characteristics of dissipative waveguides, and demonstrating the accuracy of the Coustyx solution in comparison with the analytical solution.

5 Results and Discussion

Analysis is carried out by running the Analysis Sequences defined in the Coustyx model named `Run Validation - FMM` . An Analysis Sequence stores all the user inputs specified for an analysis, such as boundary integral formulation type, frequency range and spacing, solution method, along with various requested outputs.

The results from Coustyx analysis, and the analytical solutions, are written to the output files `validation_results_fmm.txt`, `face_center_results_fmm.txt`, `corner_results_fmm.txt` for plotting using external tools.

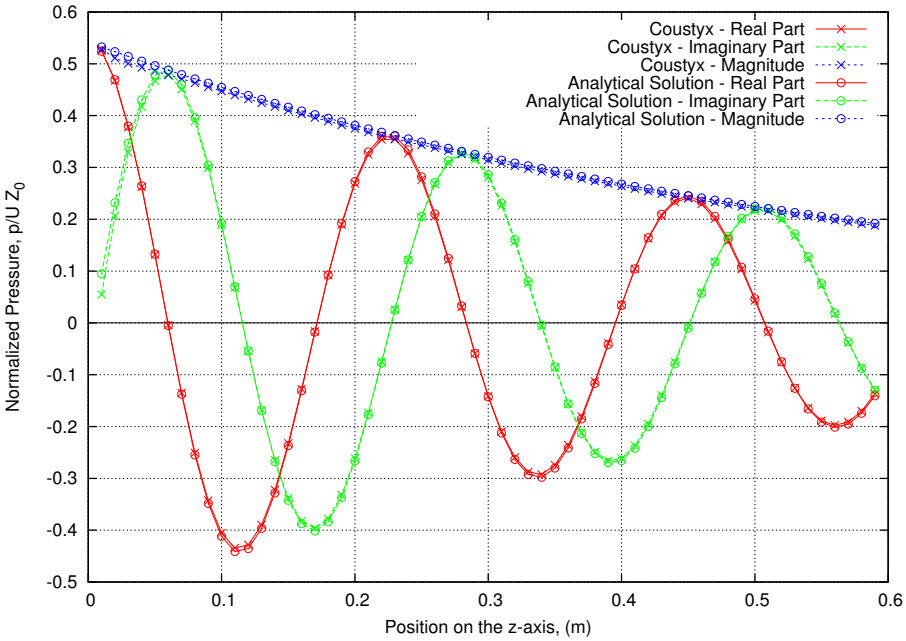

Figure 4: Variation of sound pressure with distance along the z-axis.

Figure 4 shows the variation of the sound pressure along the duct center line. The apparent wavelength in the z-direction from Figure 4 is 0.227 m that corresponds precisely to the real part of the propagation wavenumber $k_{z,0,0} = 28.06 + i1.76$ from the analytical solution as $2\pi/k_{z,0,0} = 0.223$. This result is very interesting, as the Coustyx solution was not in any way predisposed to yield this, and the surface point source distributions from the BEM solution all radiate fields with e^{ikr} spatial variation, where the wavenumber $k = \omega/c = 18.32$. For the case of the *rigid* side walls the wavelength in the z-direction would have been 0.343 m. So the apparent wavelength is *shorter* when the duct is lined with an absorbing material. From Figure 4, it is seen that the Coustyx solution is compares very well with the analytical solution, for all z

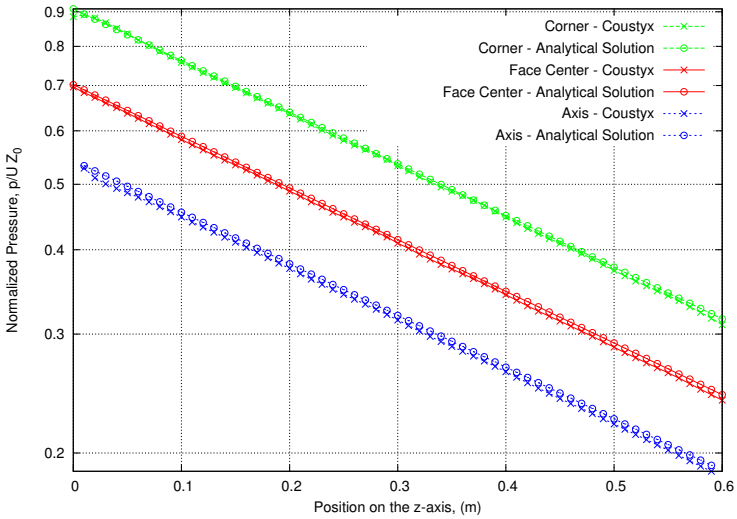

Figure 5: Magnitude of the normalized sound pressure at various points on the duct cross-section.

The sound pressure at three points on the cross-section namely – a corner point, a point on the face center, and a point on the duct axis is plotted in Figure 5. The y-axis on the graph is in log scale. From the Figure 5, it is seen that all the three curves are parallel, corresponding to an exponentially decaying variation with same attenuation rate but different starting values. Also the sound pressure level at the corner is maximum, as predicted earlier from the analytical solution.

References

[1] D. W. Herrin. Impedance model for 1-inch thick foam with rigid backing. Personal communication.

[2] Allan D. Pierce. *Acoustics, An Introduction to Its Physical Principles and Applications.* Acoustical Society of America, 1989. Pages 110-111.

[3] M. L. Munjal. *Acoustics of Ducts and Mufflers.* John Wiley & Sons, Inc., 1987. Pages 26–30, and Chapter 6.